

See discussions, stats, and author profiles for this publication at: <https://www.researchgate.net/publication/231700537>

# Molecular Design of Functionalized m-Poly(phenylene ethynylene) Foldamers: from Simulation to Synthesis

ARTICLE *in* MACROMOLECULES · JUNE 2010

Impact Factor: 5.8 · DOI: 10.1021/ma100746x

---

CITATIONS

5

---

READS

19

4 AUTHORS, INCLUDING:



[William Batson](#)

Technion - Israel Institute of Technology

11 PUBLICATIONS 10 CITATIONS

[SEE PROFILE](#)



[David A Bruce](#)

Clemson University

60 PUBLICATIONS 2,112 CITATIONS

[SEE PROFILE](#)

## Molecular Design of Functionalized *m*-Poly(phenylene ethynylene) Foldamers: from Simulation to Synthesis

Ha H. Nguyen, James H. McAliley, William R. Batson, III, and David A. Bruce\*

Department of Chemical and Biomolecular Engineering, Clemson University, Clemson, South Carolina 29634-0909

Received April 7, 2010; Revised Manuscript Received June 2, 2010

**ABSTRACT:** *m*-Poly(phenylene ethynylene)s (mPPEs) are a class of synthetic molecules being used for biocide coatings, catalysis, as well as chemical and biomolecule sensing because they exhibit a propensity to form a helical secondary structure in solution. Additionally, the folding of mPPEs into such helical arrangements may generally be controlled by varying the primary structure of the mPPE and/or the nature of the solvent. As such, several attempts have been made at developing heuristics for predicting *a priori* whether a particular mPPE will fold into a helix in a given solvent based on energetic and structural considerations. However, the experimental evidence shows that the formation of helical structures by mPPEs cannot be reliably predicted using such simple models. In this work, we demonstrate that replica-exchange molecular dynamics (REMD) simulations provide excellent agreement with experimental observations. We have simulated 20 different mPPE variations in five different solvent environments. Experimental results are available for eight of these one hundred systems, and in all eight of these cases the REMD results were in agreement with the experiments. Additionally, we simulated and then synthesized two previously unreported mPPEs having both ester and nitrile functional groups. After studying their folding behaviors in chloroform and acetonitrile, it was found that experimental results were in agreement with our predictions. This illustrates how REMD simulations, which are easily carried out with publicly available software on most modern computing systems, can be used to guide synthesis efforts focused on the formation of macromolecules with specific secondary structures.

### Introduction

The prediction and control of secondary structure in polymers has long been of interest to the scientific community, because the functions and activities of these materials can often be correlated to their structure. This has implications for a wide range of technologies, including self-assembled nanostructures, high-performance engineering materials, and biologically active molecules such as proteins and enzymes. Though considerable progress has been made in understanding secondary structure formation in these systems, in most cases the complexity of such molecules has made it difficult for a reliable, purely predictive framework to be established. Thus, many researchers have sought out simple analogs of these complex systems, to understand the fundamental science behind secondary structure formation, and to build a foundation upon which more complex frameworks may be based.

In this effort to develop new biomimetic materials and better understand secondary structure formation, Moore and co-workers<sup>1–6</sup> introduced a new class of polymers named *m*-poly(phenylene ethynylene)s (mPPEs). Some of these polymers are known to fold into an ordered, helical conformation in solution, and the process is controllable by various factors, for example solvent conditions, temperature, etc. Thus, mPPEs have the potential for use in a wide range of applications that require self-assembly (e.g., chemical sensing, biocide coatings, and catalysis), yet they also provide an interesting template for studying the fundamental interactions that govern macromolecular

conformations. The folding processes of several mPPE variations have been examined in detail by other authors,<sup>7–13</sup> and classical molecular simulation methods have proved a useful tool in such studies. Yet, to date, simulation has been used primarily as a means to study known materials, rather than as a predictive tool. In this work, we demonstrate that related methods can be successfully used in predictive studies, allowing a large combinatorial parameter space to be screened on the computer before investing laboratory resources on the synthesis and characterization of new materials.

The primary adjustable features of mPPEs are the functional groups attached to the phenylene ethynylene backbone. Our initial studies examined the structure directing effects of functional groups positioned *meta* to the polymer backbone. As shown in Figure 1, these pendant groups may take on a wide range of chemical functionality. In general, the formation of secondary structure in any given mPPE is dependent on the functionality of its side groups (labeled R in Figure 1) and the solvent in which the mPPE is placed. For example, the ester-functionalized mPPE has been experimentally proven to fold into a helical conformation in acetonitrile and other solvents, but maintains a random coil conformation in chlorinated solvents.<sup>1,14</sup>

Previous studies of helix formation by mPPEs have identified several structural factors that contribute to folding. First, the series of *m*-ethynylene linkages in the polymer backbone allows for  $\pi/\pi$  interactions to occur between aromatic groups that are 1, 7 neighbors, as shown in Figure 2. This interaction has a stabilizing effect, which is analogous to the formation of hydrogen bonds in a protein  $\alpha$ -helix. This effect may be reinforced or counteracted by other important factors, including interactions between the solvent and solvophilic or solvophobic sites along the polymer,

\*Corresponding author. Address: 127 Earle Hall, Chemical & Biomolecular Engineering Department, Clemson University, Clemson, SC 29634-0909. E-mail: dbruce@clemson.edu.

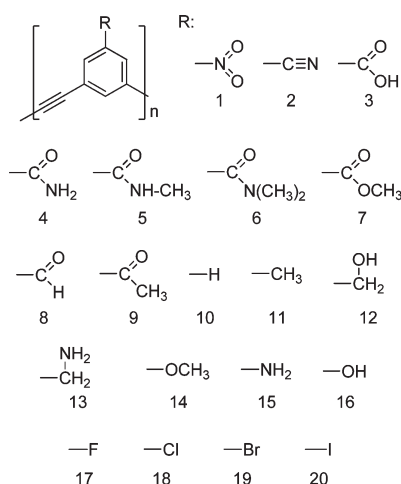


**Figure 1.** Structure of *m*-phenylene ethynylene homopolymers having one substituent group on each aromatic ring.

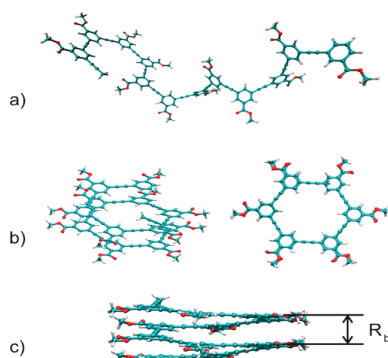


**Figure 2.** Typical conformations of mPPEs. This figure shows the ester mPPE ( $R = 7$ ) in (a) a random extended conformation, and in a helical conformation as viewed (b) axially and (c) perpendicular to the helical axis. The interlayer spacing equals  $R_b$ , and atom colors for oxygen, hydrogen and carbon are red, white and blue, respectively.

and the presence of electron withdrawing or donating groups attached to the aromatic rings.<sup>2,5</sup> Continuing with our previous example, the folding preference of the ester-functionalized mPPE in acetonitrile has been attributed to a combination of these three factors: the solvophilic nature of its ester side groups, the solvophobic nature of the polymer backbone, and the electron-withdrawing character of the ester groups on the aromatic rings. Because the compact helix exposes the mPPE side groups to solvent, while shielding the polymer backbone, the helix conformation is quite stable from the perspective of polymer/solvent interactions. Further, it has been argued that electron-withdrawing groups, such as esters, on the aromatic rings serve to strengthen the  $\pi$ -stacking interactions within the polymer, adding more stability to the helix.<sup>2,15</sup>

The above explanation is certainly adequate to justify the observed folding behavior of an ester-functionalized mPPE, which possesses a folding bias in many solvents.<sup>14</sup> However, such reasoning is not sufficient to establish a reliable set of heuristics for predicting folding behavior *a priori*, since the competing effects of solvophilic/solvophobic interactions and  $\pi$ -stacking interactions are not easily quantified. For example, the conventional argument asserts that electron donating substituents on the aromatic rings should weaken  $\pi$ -stacking interactions, and therefore, favor the unfolded state; this was offered as a reason why an mPPE with electron-donating groups did not fold in acetonitrile

and other polar solvents.<sup>2</sup> However, a water-soluble, folding mPPE with electron donating functional groups was successfully synthesized,<sup>16</sup> contrary to these heuristics. Indeed, the effect of electron donating/withdrawing groups itself is not clearly understood, as the  $\pi$ -stacking phenomenon is due to a combination of effects, such as exchange repulsion, induction and dispersion.<sup>17–21</sup> Experimental evidence and high level quantum calculations have even suggested that *all* functionalized aromatic structures have stronger  $\pi$ -stacking interactions than normal benzene rings,<sup>18,19,21–23</sup> indicating that both activating and deactivating functional groups could stabilize mPPE helical structures through their effect on  $\pi$ -stacking interactions.

Further complications arise when considering the effect of solvophobic/solvophilic sites on an mPPE polymer's native conformation. Naturally, these definitions will depend on the characteristics of the solvent, and therefore, the choice of solvent has a direct effect on the formation of secondary structure. For example, studies of the ester mPPE in different solvents indicate that certain solvents—chloroform, dichloromethane and tetrahydrofuran—do not favor the folded conformation, while other solvents—acetonitrile and hexane—do favor the helix. The stability of extended conformations in chlorinated solvents was explained as the result of strong CH/ $\pi$  interactions between the exposed aromatic rings and solvent molecules.<sup>14,21,24</sup> Thus, when chloroform is used as the solvent, the polymer backbone exhibits some solvophilic character. Yet, the effect of solvent upon folding is not easily separated from the effects of side group functionality. For example, methanol induces folding in the ester functionalized mPPE,<sup>14</sup> while the same solvent promotes extended conformations for another mPPE having electrolytic side groups.<sup>16</sup>

Though some of the science behind the folding driving force in mPPEs remains unsettled, we note that there have been several successful studies which examined the folding process of mPPEs by classical simulation methods, such as molecular dynamics (MD).<sup>7–13</sup> For example, the MD results of Elmer et al. show that the folding time of mPPEs generally vary from 70 to 400 ns, and this is in agreement with experimental results.<sup>12</sup> In another study, the same authors conducted MD simulations of ester functionalized mPPEs dissolved in four different explicit solvents—acetonitrile, methanol, chloroform and water—to quantify the time required for secondary structure formation.<sup>13</sup> When chloroform and water were used as a solvent, no folding event was witnessed; therefore, it was concluded, that chloroform hindered the folding ability of ester mPPEs, and that the folding process in these solvents would only occur over long time scales, if at all.<sup>13</sup> This result agrees with experimental data, in which no folding was observed in chloroform.

The aforementioned simulation studies demonstrate a favorable comparison between classical models and experimental evidence. Yet, for the purpose of determining the most favored conformation, the procedure of running a single MD simulation initialized from a random extended state is by itself unable to provide positive proof of the preferred conformation. For example, failure to observe the folding process in such simulations is insufficient evidence that the folded state is unfavorable, because the time scale for the folding process might simply be longer than the simulation time for a given initial polymer configuration. Thus, while conventional MD simulations are ideal for examining folding *rates*, they are not well suited for the purpose of this study—determining whether the helical conformation is favored for a given mPPE/solvent pair.

Adisa and Bruce used two enhancements to the conventional MD approach in their study of mPPEs,<sup>8</sup> resulting in a method specifically designed to determine the native state of mPPEs in solution. The first enhancement was the use of replica exchange molecular dynamics (REMD)<sup>25</sup> rather than conventional MD. The REMD technique is a hybrid method that incorporates both

Newtonian dynamics and Monte Carlo (MC) concepts, and it is well-suited for use with modern parallel computing architectures. Compared to a conventional MD simulation, REMD converges much more quickly to the thermodynamically favored state of the system,<sup>25–29</sup> allowing the native state to be reached in significantly less simulation time. As a second enhancement, a procedure was used in which two simulations were carried out for each mPPE in solvent: one beginning with an extended initial conformation, and the other with a helical initial conformation. Using results from both starting points, a more decisive conclusion may be reached regarding the native conformation of the system. The authors modeled two mPPE variations with this technique, one with ether and the other with amine side chains, in explicit water. Simulation results indicated that, for both the ether and amine functionalized mPPEs, helix formation is likely to occur in water.<sup>8</sup> Though the incorporation of replica exchange moves in REMD makes the technique unsuitable for studying kinetics, these results demonstrate that the method is effective in determining the favored conformation of a given mPPE in solution.

In the present study, a similar protocol was used as a simple, quick test for screening the folding behavior of over 100 different mPPE/solvent combinations. This procedure was first validated against the previously reported experimental data. It was then used to predict the structure of two new variations of mPPEs, which were later synthesized and characterized to confirm the REMD predictions. We then employed this method in a large-scale combinatorial investigation, over a wide range of mPPEs with different functional groups in several solvent conditions. These combined simulation–synthesis efforts clearly show the predictive capabilities of the REMD method and illustrate how these simulations can be used to significantly reduce, if not eliminate, trial and error synthesis efforts focused on the production of ordered organic molecules.

## Methods

**Simulation Procedure.** All simulations were conducted using Gromacs, version 3.3.1.<sup>30–36</sup> The initial mPPE structures were generated using Material Studio 4.0.<sup>37</sup> The procedure for preparing and minimizing the solvated box was similar to that reported by Adisa and Bruce.<sup>7,8</sup> All bond lengths in the polymers were held constant using the LINCS algorithm.<sup>35</sup> The solvated boxes were equilibrated using isothermal–isobaric (*NPT*) molecular dynamics for 200 ps, with Berendsen temperature coupling<sup>38</sup> ( $T = 300$  K,  $\tau_T = 0.1$  ps) and Parrinello–Rahman pressure coupling<sup>39</sup> ( $P = 1$  bar,  $\tau_P = 1$  ps). The resulting equilibrated systems were then used as the initial structures for REMD simulations at constant volume (*NVT*).

To determine the preferred structure of each mPPE, two REMD simulations were performed: one beginning with the polymer in a random extended conformation, and the other beginning with a helical conformation. For the first simulation, the conformation of the molecule is not uniquely defined, since the extended state is essentially random. Yet, preliminary tests showed no significant difference in the folding behavior of the ester mPPE after running multiple REMD simulations initialized from ten unique conformations. Therefore, for all remaining mPPEs, only one random extended conformation was used. Thus, we found that two simulations—one beginning with a random structure and the other beginning with a helical structure—are sufficient to determine whether a given mPPE is likely to take on a helical or random extended structure in a studied solvent condition.

**REMD Simulation Parameters.** REMD simulations were conducted using a temperature range of 300–600 K. The

**Table 1. Solvents Considered in This Study**

solvent	isothermal compressibility <sup>a</sup> ( $\times 10^5$ bar <sup>-1</sup> )
acetonitrile	10.7
chloroform <sup>b</sup>	11.28
diethyl ether	20.90
methanol	12.93
ethanol	11.91
hexane	17.09
carbon tetrachloride <sup>b</sup>	11.28
acetone	12.23

<sup>a</sup>Compressibilities taken from Lide and Kehiaian<sup>49</sup> and Torres et al.<sup>50</sup> <sup>b</sup>All-atom models (others are united-atom models).

temperature distribution and the number of replicas were selected based on the procedure described by Adisa and Bruce,<sup>7,8</sup> such that the exchange probabilities in all simulations were approximately 15% to 20%. This is necessary for an efficient convergence toward the true ensemble average.<sup>8,27,29,40</sup> A time step of 2 fs was used, with replica exchange moves attempted every 0.5 ps (250 steps). The length of each REMD simulation was kept at 10 ns. The other simulation parameters used here were identical to those reported earlier.<sup>8</sup> Twin range cut-offs were used for van der Waals and Coulomb interactions, each with a cutoff radius of 1.2 nm; neighbor lists were updated every 10 steps; trajectories and energy terms were saved every 5000 steps.

Though a range of temperatures are examined in REMD simulations, only the trajectories at 300 K were used in our analysis, representing the mPPEs structures at ambient temperature. Graphical representations of mPPE structures were obtained with visual molecular dynamics.<sup>41</sup> To evaluate the level of order in mPPE conformations during REMD simulations, the following parameters were calculated: the radius of gyration ( $R_g$ , nm), the solvent accessible surface area<sup>42,43</sup> (SASA, nm<sup>2</sup>), the Lennard-Jones interaction potential between mPPE atoms ( $V_{LJ,P-P}$ , kJ/mol), the Lennard-Jones interaction between mPPE and the solvent molecules ( $V_{LJ,P-S}$ , kJ/mol), and the distance between two overlapping aromatic rings ( $R_b$ , nm) as defined in Figure 2c.<sup>33</sup> Because of the similarity in time evolution of these five parameters, they were reported only with the first two results. Subsequently,  $R_g$  was selected as the preferred order parameter. All simulations were conducted using the *Palmetto* supercomputer, maintained by the high-performance computing group at Clemson University.<sup>44</sup>

**mPPE Model.** The atom types, bonded and nonbonded parameters for the mPPE models were taken directly from the optimized potential for liquid simulations (OPLS),<sup>45–47</sup> as distributed with Gromacs 3.3.1, with modifications for dibenzyl ethynylene dihedral parameters.<sup>7</sup> A polymer chain length of 12 monomers (12 aromatic rings) was selected, based on the length required for a stable helical structure in experimental studies.<sup>1,4</sup> To simplify the model, the long solvophilic pendants used in experimental studies<sup>1</sup> were excluded, based on evidence that their role in mPPE folding behavior is likely negligible.<sup>12,13</sup> In experimental studies, the lengths of those solvophilic tails were designed to facilitate solvation of the mPPEs, and this consideration is less important for molecular simulations since a single polymer chain may be placed directly in solvent when defining the simulation cell.

The mPPE models were built based on the procedure described earlier.<sup>7,8</sup> The extended structures were built by randomly assigning torsion angles (dibenzyl ethynylene torsion angle), and the helical structures were built by manually adjusting dihedral angles in the extended structure until a helical conformation was obtained. In constructing the



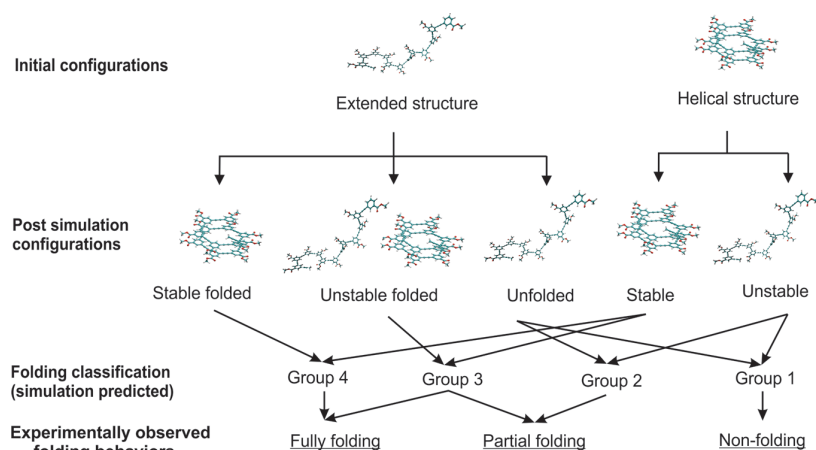


**Figure 3.** Classification of REMD simulation outcomes for mPPE polymers, shown with the corresponding folding behaviors most likely to be observed in experiments.

helices, the distances between two overlapping aromatic rings were set at 0.35 nm, following the optimum distance of  $\pi/\pi$  interactions in benzene and its functionalized derivatives.<sup>18,21,48</sup> In total, 20 mPPEs were built for the combinatorial portion of this study, using the functional group variations shown in Figure 1.

**Solvent Models.** Eight solvents were considered in this study. These were selected to represent a range of electronic characteristics, from highly polar to nonpolar. Table 1 lists these solvents and their isothermal compressibilities.<sup>49,50</sup> Models for these molecules were also taken from the OPLS all atom (AA) and united atom (UA) force fields.<sup>45</sup> In all *NPT* simulations, the listed experimental compressibilities were used for defining the pressure coupling time constant  $\tau_p$ , with arithmetic averages used for bicomponent mixtures. All solvents, except chloroform, were represented by united atom models that effectively combined aliphatic hydrogens and their respective carbon atom into a single pseudo atom. In this study, the ester mPPE ( $R = 7$ ) was simulated in all eight solvents, as well as in three mixtures of acetonitrile and chloroform, as a means of validating the modeling approach against existing experimental data. Other mPPEs were simulated in five solvents: chloroform, acetonitrile, acetone, diethyl ether and hexane. We note that the UV absorbance of acetone does not allow an effective spectroscopic study of folding; thus, the simulation results presented in this work provide a means to investigate the folding behavior of mPPEs in this type of solvent, a task which would otherwise be difficult to accomplish.

## Results and Discussion

The REMD simulation results for each mPPE were found to fall under one of four classifications. As indicated in Figure 3, there are several possible outcomes for each pair of simulations. If the favored state of the mPPE is unfolded, the simulation initialized from the folded state will show an increase in  $R_g$  upon unfolding, while  $R_g$  will remain relatively constant in the simulation initialized from the unfolded state. We refer to this scenario as group 1. Alternatively, the REMD simulation with an unfolded initial state may show a decrease in  $R_g$  and occasionally form a helix without maintaining the structure for any long period of time. This indicates the helix is slightly stable but not the preferred state, and we refer to this scenario as group 2. In a third scenario, group 3, the simulation beginning from the helical conformation remains helical during the entire simulation, while

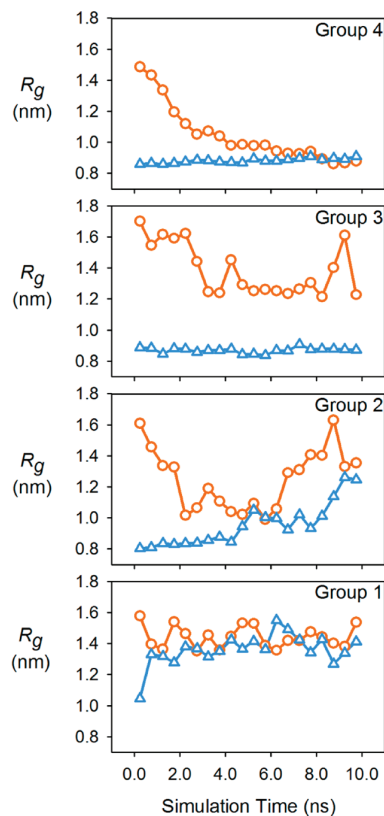


**Figure 4.** Radius of gyration data for examples of the different classifications of mPPE simulation results: group 4 (stable helical conformation,  $R_g = 0.8\text{--}1.0$  nm), group 3 (helical conformation is observed for extended periods, but may not be the only low energy conformation), group 2 (helical conformation is one of many observed conformations), and group 1 (stable unfolded state,  $R_g > 1.2$  nm). Circles indicate simulations beginning from a random coil, and triangles indicate simulations beginning from a helical conformation. Data points are time averages over 500 ps.

the one initialized with the unfolded structure never forms a stable helix (though helical conformations may be sampled briefly during the simulation). The distinction between groups 2 and 3 is that the helix is much more stable in group 3 than in group 2. Further, simulation results in group 3 are sufficient to

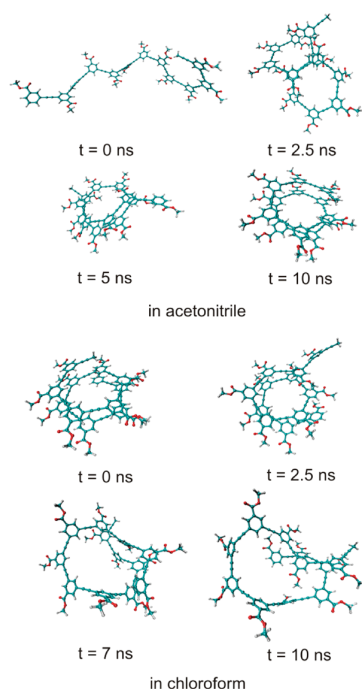


**Figure 5.** Representative conformations at 300 K during REMD simulation of the ester-functionalized mPPE ( $R = 7$ ), observed at various simulation times. Conformations in acetonitrile were taken from a simulation initialized from a random coil, while the conformations in chloroform were taken from a simulation initialized from a helical conformation. Atom colors for oxygen, hydrogen, and carbon are red, white, and blue, respectively.

indicate folding, though formally no conclusion may be drawn between fully folding and partially folding. As a fourth possibility, the unfolded polymer may progress to a stable helix during the simulation, while the simulation starting from the helix remains unchanged. This scenario clearly indicates the helix is the preferred conformation, and is labeled group 4. Thus, in this classification system, each mPPE/solvent pair is given a number from 1 to 4, with 1 indicating the least likelihood of the mPPE polymer folding into a helical conformation and 4 the greatest. Representative time evolutions of  $R_g$  for these four groups are shown in Figure 4.

Note that group 3, as defined in Figure 3, is technically inconclusive to determine the favored structure of the relevant mPPE. If  $R_g$  remains relatively constant in both types of REMD simulations, even if several folded states were sampled in the simulation initialized with an extended mPPE structure, this is most likely an indication that the simulations have simply not run long enough to observe the progression to the preferred state. Still, it is clear that the helical conformation is significantly more stable for species ascribed to group 3 as compared to those in group 2, and therefore, we may assert that for an mPPE/solvent system in group 3, folding is likely but not certain.

**The Folding Behavior of Ester mPPE ( $R = 7$ ).** The most extensively studied mPPE that exhibits a tendency to fold into a helical conformation is the ester-functionalized mPPE. Its folding behavior has been experimentally characterized in many different solvents, including acetonitrile and chloroform.<sup>1,14</sup> In this section, our simulation protocol was verified against these experimental results, using an analogous structure ( $R = 7$ , see Figure 1). The results serve as justification that the simulation procedure used in this study is adequate to evaluate mPPE folding behaviors.

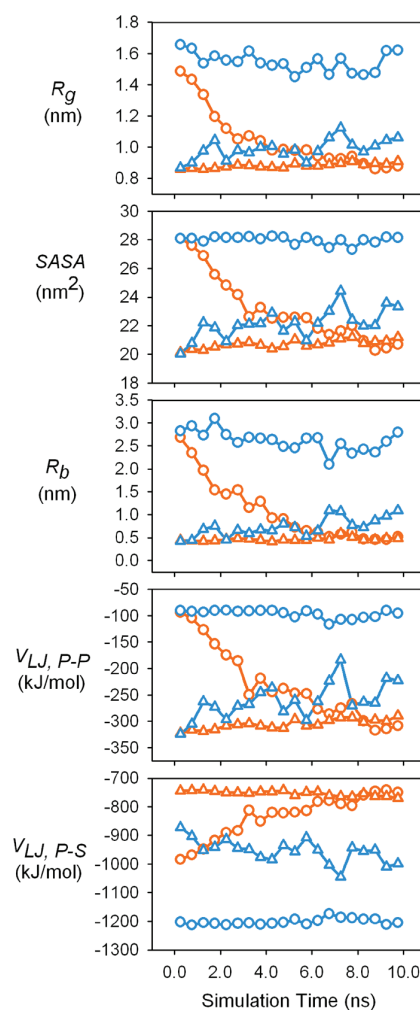


**Figure 6.** Evolution of folding indicators during REMD simulations of the ester-functionalized mPPE ( $R = 7$ ) in acetonitrile (orange series) and chloroform (blue):  $R_g$ , radius of gyration; SASA, solvent-accessible surface area;  $R_b$ , phenyl ring separation distance;  $V_{LJ, P-P}$ , polymer/polymer Lennard-Jones energy;  $V_{LJ, P-S}$ , polymer/solvent Lennard-Jones energy. Circles indicate simulations beginning from a random coil, and triangles indicate simulations beginning from a helical conformation. Data points are time averages over 500 ps.

Simulation results for the ester mPPE in acetonitrile and in chloroform fell under groups 4 and 1, respectively, in agreement with experimental observations: the ester mPPE formed a helical conformation in acetonitrile and a random extended structure in chloroform. Simulation results are represented by the visual snapshots of the trajectories in Figure 5. Further results are given in Figure 6, which shows the time evolutions of the  $R_g$ , SASA, the Lennard-Jones interactions and the  $\pi$ -stacking distance  $R_b$ .

The REMD simulation beginning with the extended structure of the ester-functionalized mPPE in acetonitrile indicated that the oligomer formed a stable and well-defined helical conformation. The steadily decreasing  $R_g$  and SASA indicate the transformation from the extended structure to a more compact conformation, which is also supported by the change in the Lennard-Jones interactions. The intramolecular Lennard-Jones energy of the polymer,  $V_{LJ, P-P}$ , became increasingly negative, reflecting an increase in the number of close contacts between segments of the polymer chain. Meanwhile, the polymer/solvent Lennard-Jones energy,

$V_{LJ,P-S}$ , became less negative, indicating less interactions between the polymer's atoms and solvent molecules. All five parameters became stable after 5 ns, indicating that the compact helix is likely the favored structure. This includes the order parameter  $R_p$ , which became nearly constant after 5 ns, confirming the formation of an ordered, defined structure. When the simulation was initialized with a helical conformation, we observed a stable structure, with only small deviations in all five monitored values over the entire 10 ns simulation. Thus, both simulations indicate that the helix is the thermodynamically favored conformation in acetonitrile.

The above results are sufficient to place the ester mPPE/ acetonitrile system in group 4, according to the classification system defined in Figure 3. We note that, in the REMD simulation beginning with an extended structure, the helical conformation was observed as early as 3 ns, becoming stable after 5 ns of simulation time. Compared to the 200 to 400 ns folding time required in regular MD,<sup>12,13</sup> this is a significant speedup—even after factoring in the number of extra processors required for the higher temperature replicas in REMD. Because of the accelerated sampling achieved by replica exchange moves, folding times quoted for the REMD results do not correspond to real folding time scales as they do in the conventional MD results; there is evidence that mPPEs typically do take hundreds of nanoseconds to fold.<sup>51</sup> Yet, in quoting these numbers, we simply wish to demonstrate that REMD requires significantly less computational resources than MD to arrive at the thermodynamically favored state.

Further observations confirm the efficiency of REMD in terms of conformational sampling. Before reaching the final helical conformation in acetonitrile, our simulations of the ester mPPE sampled multiple intermediate states similar to those that occurred during a regular MD simulation reported in earlier studies.<sup>12,13</sup> These intermediate states do not represent the actual pathway or time scale necessary to form a helical conformation from an extended structure, as would be obtained from conventional MD,<sup>12,13</sup> yet their occurrence implies that the REMD method achieves efficient sampling of the canonical phase space distribution, which is necessary for converging toward the most stable structure.

In contrast to the steady collapse of the extended structure of the ester mPPE in acetonitrile, our simulations show the extended structure was stable in chloroform. The monitored parameters shown in Figure 5 indicate the extended structure did not become more compact in this solvent, suggesting the random extended conformation is favored. This observation was further supported by results from the simulation beginning with the helical structure, in which the helix became unstable and unfolded (see Figure 6). An unfolded structure was observed shortly after the beginning of the simulation, at 1.5 ns. From that point the mPPE alternated between helical and random extended structures with increasing frequency over time, becoming a fully opened structure at the end of the simulation. Thus, we conclude that the favored state is the unfolded random extended structure, and categorize this system in group 1. These results clearly show the agreement between REMD simulation results and experimental results<sup>1</sup> regarding the folding behavior of ester functionalized mPPEs in pure acetonitrile and pure chloroform.

The results in Figure 6 show that our selected conformational indicators are closely correlated with each other, and also with the visual depictions of conformations in Figure 5. Thus, although all five parameters were examined in each of the following REMD simulations, we have selected the

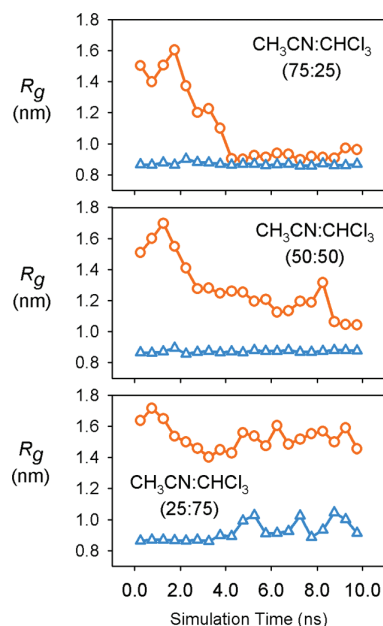


**Figure 7.** Time evolution of the radius of gyration ( $R_g$ ) of the ester-functionalized mPPE ( $R = 7$ ) at 300 K, observed during REMD simulations of varying solvent composition (volume ratios listed in insets). Results in pure acetonitrile and in pure chloroform are given in Figure 6. For each solvent condition, two REMD simulations were performed: one initialized with the helical conformation (blue triangles) and another initialized with a random configuration (orange circles). Each plotted data point is a time average over 500 ps, placed at the center of the corresponding time interval.

radius of gyration ( $R_g$ ), as the preferred indicator for all remaining plots.

Simulation results for the ester-functionalized mPPE ( $R = 7$ ) using mixtures of acetonitrile and chloroform (25%, 50%, and 75% acetonitrile by volume), demonstrated a qualitative correlation between the stability of the mPPE helical structure and the concentration of acetonitrile (Figure 7). It can be seen that, upon increasing the chloroform concentration, the amount of simulation time required for the extended mPPE structure to become folded increases, with mPPEs in mixtures greater than 50% chloroform never reaching the folded state. At 75% chloroform, the simulation of the helical structure begins to show signs of instability, with the extended structure clearly favored in pure chloroform. These observations are in agreement with the experimental results reported earlier.<sup>1</sup>

Simulation results also showed that the ester mPPE folded in other solvents, including methanol and carbon tetrachloride (Figure 8). This folding bias is consistent with published experimental results.<sup>14</sup> The ester mPPE also folded well in acetone, providing the first evidence that the ester mPPE will form a helical secondary structure in this type of solvent. Simulation results also showed that ester mPPEs are likely to fold in diethyl ether, ethanol and hexane, although experimentally the polymer does not dissolve appreciably in these solvents.<sup>14</sup> Because the ester mPPE simulated in this study has short ester side chains, and the simulation systems consisted of only one mPPE molecule, these results provide evidence suggesting that the long-tailed solvophilic pendants do not play a significant role in the helix formation process. Instead, their function is primarily to increase the solubility of the ester mPPE, as suggested elsewhere.<sup>1,52</sup> These results also provide justification for our choice to exclude the long

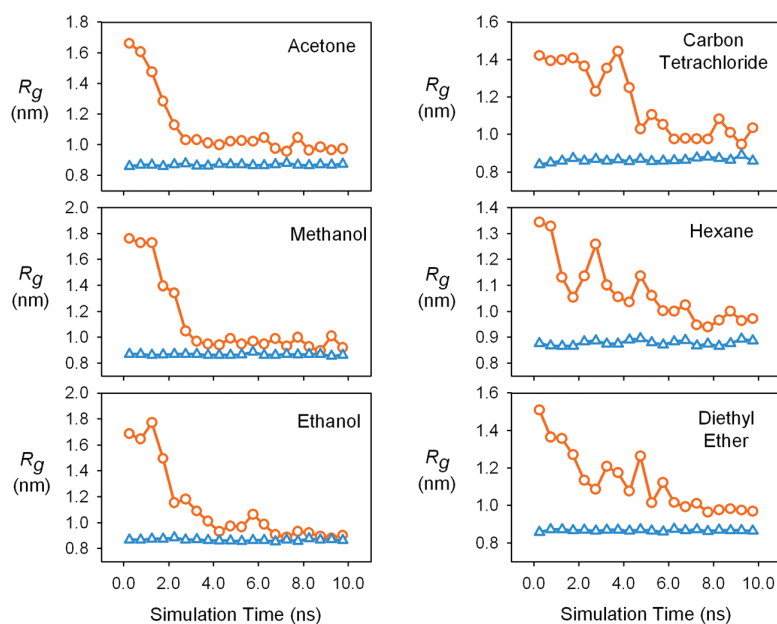


**Figure 8.** Time evolution of the radius of gyration for the ester-functionalized mPPE ( $R = 7$ ) in various solvents. Orange circles denote simulations starting from a random coil, whereas blue triangles denote simulations starting from a fully folded helical structure. Each plotted data point is a time average over 500 ps, placed at the center of the corresponding time interval.

solvophilic pendants in the ester mPPE structures in this study.

Although the solvents were selected to investigate the effect of their polarity on the folding behavior of ester mPPE, no clear difference was observed. The helical structures of the ester mPPE were stable in all selected solvents, except chloroform. The extended structures appeared to follow the similar overall change from initial structures into the final coiled conformations, though there were minor qualitative differences, which could be attributed to the selection of initial configurations and the number of atoms in each simulation. Similar to acetonitrile, methanol seemed to be a better solvent for inducing folding in the ester mPPE than carbon tetrachloride, as suggested by Hill and Moore.<sup>14</sup>

The helical structures in our simulations have overlapping aromatic rings that are separated by an average distance ( $R_b$ ) of 0.45 nm, in the range of the optimal  $\pi$ -stacking distance of aromatic rings. This is in reasonable agreement with other high level quantum simulations<sup>18,21,48</sup> and experimental data,<sup>53,54</sup> demonstrating that structurally, the helical conformations in our simulations closely resemble those of synthesized mPPEs. This also provides further evidence that the weak  $\pi$ -stacking interactions are well described by the semiempirical OPLS force field,<sup>45,55</sup> justifying our use of the OPLS force field to simulate mPPE systems.

**Validation against New Experimental Results.** After obtaining favorable comparisons between our simulation results and the previously available data for the ester mPPE, we sought to test the predictive capability of our REMD simulation protocol. This was accomplished by simulating and then synthesizing two new variations of mPPEs. As shown in Figure 9, molecules 21 and 22 are more complex than those depicted in Figure 1, with up to three different functional groups on each chain. In both molecules, the ester ( $-\text{COOTg}$ ,  $\text{OTg} = \text{triethylene glycol}$ ) and nitrile ( $-\text{CN}$ ) functional groups were arranged in an alternating pattern in the position *meta* to the ethynylene linkages, while in molecule 21 an ether ( $-\text{OCH}_3$ ) functional group was additionally

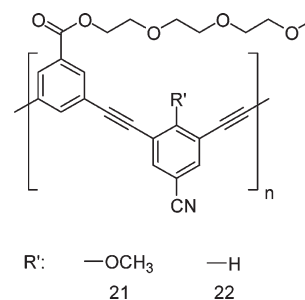


**Figure 9.** Structure of the mPPEs synthesized for experimental validation of the simulation protocol.

positioned *para* to each nitrile group. Thus, when folded into a helix, both molecules have ester and nitrile groups exposed along their outer surface, while molecule 21 has the additional ether groups inwardly oriented inside the helical cavity. These polymers were selected because they have been previously unreported in the literature and are easily synthesized using a Sonogashira polymerization technique, which has been used previously to prepare similar mPPEs.<sup>56</sup> Further, the presence of the additional functional groups in the ester functionalized mPPE backbone allowed us to study their impact on the solubility and folding characteristics of the polymer.

The folding behaviors of molecules 21 and 22 were simulated and measured in chloroform and acetonitrile. REMD simulation results showed that 21 and 22 were both categorized in group 1 in chloroform and group 3 in acetonitrile. These results indicate the mPPEs should not fold in chloroform, but should at least partially fold in acetonitrile. The UV and fluorescence spectra for the synthesized mPPEs, shown in Figure 10, support these assertions: when changing the solvent from chloroform to acetonitrile, the absorbance at 305 nm (molecule 21) and 307 nm (molecule 22) decreased, indicating more *cisoid* conformations. In the fluorescence spectra, the absence of a peak at 380 nm (molecule 21) and 350 nm



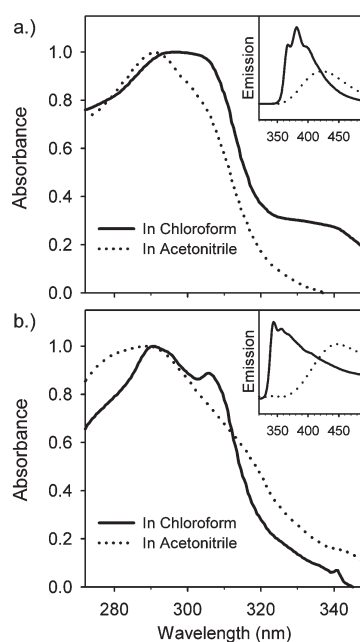


**Figure 10.** UV absorbance (normalized) and fluorescence spectra (insets) as measured for (a) molecule 21 and (b) molecule 22, in chloroform and acetonitrile solvents.

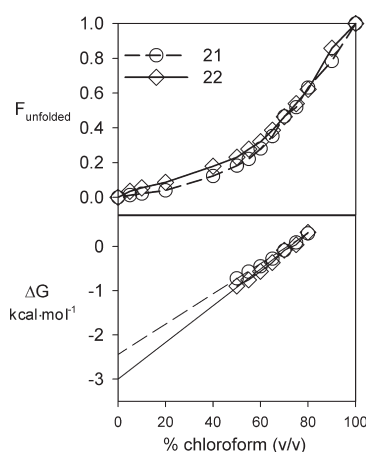


**Figure 11.** Fraction of mPPEs 21 and 22 that exist in an unfolded conformation,  $F_{\text{unfolded}}$ , and  $\Delta G$  for folding from denaturation titration experiments for molecules 21 and 22.

(molecule 22) and the presence of a peak at 425 nm (molecule 21) and 450 nm (molecule 22) can be taken as indicators of a helical structure in acetonitrile.<sup>1</sup> From these observations, we conclude that these two mPPEs in acetonitrile are experimentally categorized as group 4 systems.<sup>1</sup> However, data from REMD simulations in acetonitrile only placed them in group 3, suggesting that their helical conformations are possibly less stable than that of the ester mPPE.

To quantify this comparison, denaturation titration experiments<sup>57</sup> for molecules 21 and 22 were conducted (Figure 11, also see additional details in Supporting Information). From these experiments, the free energy difference between the folded and unfolded states in acetonitrile ( $\Delta G_{\text{folding,CH}_3\text{CN}}$ ) and the percentage of chloroform in the mixture ( $C_{\text{CH}_2\text{Cl}_2,50}$ ) at which 50% of mPPE molecules are in an unfolded state were calculated (see Table 2). Compared to the ester mPPE,<sup>57</sup> whose 18-mer structure (having 18 aromatic rings) has a folding

**Table 2.** Denaturation Titration of Molecules 21 and Molecules 22

molecules	21	22
$C_{\text{CH}_2\text{Cl}_2,50}$ <sup>a</sup>	73	72
estimated average number of aromatic rings or $2n$	20	42
$\Delta G_{\text{folding,CH}_3\text{CN}}$ , kcal·mol <sup>-1</sup>	-3.0	-2.4

<sup>a</sup> Volume percentage of chloroform in an acetonitrile mixture at which 50% of the mPPE molecules are in an unfolded state.

$\Delta G_{\text{folding,CH}_3\text{CN}} = -7.1$  kcal·mol<sup>-1</sup>, the calculated  $\Delta G_{\text{folding,CH}_3\text{CN}}$  and the estimated number of aromatic rings for molecules 21 and 22 reveal that their helical structures in acetonitrile are less stable than that of the ester mPPE, in agreement with simulation result.

**Combinatorial Simulation Study.** In addition to the ester-functionalized mPPE ( $R = 7$ ) and molecules 21 and 22, 19 other mPPE variations (see Figure 1) were simulated in chloroform, acetonitrile, acetone, diethyl ether, and hexane. The REMD simulation results, including those of the ester mPPE, are compiled in Table 3.

The results in Table 3 show an excellent agreement between the simulated folding behaviors of mPPEs and the available experimental data for similarly functionalized mPPEs. Experimental results have been previously published for eight of the one hundred entries in Table 3, for the mPPEs with  $R = 7$ , 12, 13, and 14 in acetonitrile and chloroform, and additionally for  $R = 7$  in hexane. Of these data, referenced in the footnotes of Table 3, two mPPE/solvent combinations resulted in helical secondary structure formation, one resulted in partial folding behavior, and six indicated no secondary structure. All of these observations are in accord with our simulations results.

Also reflected in the simulation data is the general difficulty in separating the competing effects of solvophobic/solvophilic interactions and  $\pi$ -stacking strength. While some general trends were evident with respect to these factors, as will be discussed shortly, notable exceptions appeared in every case. The many exceptions are likely attributable to other factors that are less intuitive but equally important, such as site-specific interactions and entropic contributions to the solvation free energy. Such factors are incorporated naturally into the REMD simulations, and are indeed one of the major advantages to using molecular simulation in lieu of heuristics.

When examining trends with respect to solvophobic/solvophilic interactions, a common point of interest is the polarization of the solvent and solute. The conventional wisdom is that polar solvents tend to have favorable interactions with polar solutes, while nonpolar solvents form more favorable solutions with nonpolar solutes. In the context of mPPEs, this argument suggests that helix formation should be stabilized for mPPEs where the pendant groups have similar polarization to the solvent, since in the helix these groups form an outer layer that shields the polymer backbone from the solvent. Likewise, one would expect helix formation to be destabilized by weakly polar and nonpolar solvents, as these should have more favorable interactions with the polymer backbone. Yet, although 20 different functional groups were selected to represent a broad range of polarization and dielectric constants, no consistent trend was observed when attempting to correlate the polarity of the solvents and functional groups with the folding behaviors of their respective mPPEs.

For two of the strongly polar functional groups, nitrile and carboxylic acid, REMD simulations predict that secondary structure formation is inhibited by hexane. This is consistent with the conventional heuristic regarding polarization, outlined above, which indicates that folding should not be likely in such a case. However, the majority of our results indicate

**Table 3. Functionalized mPPE (see Figure 1) Folding Behaviors in Different Solvents, As Predicted by REMD Simulations<sup>a</sup>**

Functionalized mPPEs <sup>b</sup>		Folding behaviors in different solvents				
		Chloroform	Acetonitrile	Acetone <sup>c</sup>	Diethyl ether	Hexane
-NO <sub>2</sub>	( <i>R</i> = 1)	1	2	2	2	2
-CN	( <i>R</i> = 2)	1	2	2	2	1
-COOH <sup>h</sup>	( <i>R</i> = 3)	1	3	3	3	2
-CONH <sub>2</sub>	( <i>R</i> = 4)	3	3	3	4	4
-CONHCH <sub>3</sub>	( <i>R</i> = 5)	1	3	3	3	4
-CON(CH <sub>3</sub> ) <sub>2</sub>	( <i>R</i> = 6)	1	2	3	4	4
-COOCH <sub>3</sub>	( <i>R</i> = 7)	1(1) <sup>d</sup>	4(4) <sup>d</sup>	4	4	4(4) <sup>e</sup>
-CHO	( <i>R</i> = 8)	1	2	3	3	3
-COCH <sub>3</sub>	( <i>R</i> = 9)	1	2	3	3	3
-H	( <i>R</i> = 10)	1	1	1	1	1
-CH <sub>3</sub>	( <i>R</i> = 11)	1	1	1	1	1
-CH <sub>2</sub> OH	( <i>R</i> = 12)	1(1) <sup>f</sup>	2(2) <sup>f</sup>	2	3	4
-CH <sub>2</sub> NH <sub>2</sub>	( <i>R</i> = 13)	1(1) <sup>g</sup>	1	2	2	2
-OCH <sub>3</sub>	( <i>R</i> = 14)	1(1) <sup>f</sup>	1(1) <sup>f</sup>	1	2	2
-NH <sub>2</sub>	( <i>R</i> = 15)	1	1	1	1	2
-OH	( <i>R</i> = 16)	1	1	1	1	2
-F	( <i>R</i> = 17)	1	1	1	1	1
-Cl	( <i>R</i> = 18)	1	1	1	3	3
-Br	( <i>R</i> = 19)	1	3	3	3	3
-I	( <i>R</i> = 20)	1	3	4	4	2

<sup>a</sup> Where possible, experimental results for mPPEs of similar functionality are reported in parentheses. <sup>b</sup> The functional groups are placed in decreasing order of deactivating effect, from -NO<sub>2</sub> (*R* = 1) to -COCH<sub>3</sub> (*R* = 9); in increasing order of activating effect from -H (*R* = 10) to -OH (*R* = 16); the halide functional groups (*R* = 17–20) are placed separately because they have weak deactivating effects but still direct substituents to *ortho* and *para* positions in substitution reactions on the benzyl ring.<sup>58</sup> <sup>c</sup> No experimental result is listed for mPPEs in acetone, because its UV absorbance prevents measurement of UV and fluorescence spectra. <sup>d</sup> Based on the ester mPPE with long ether tails studied by Nelson et al.<sup>1</sup> <sup>e</sup> The ester mPPE with long alkyl tails was shown to fold in hexane by Brunsveld et al.<sup>59</sup> <sup>f</sup> An mPPE with equivalent functional groups showed similar behaviors in the study by Lahiri et al.<sup>2</sup> <sup>g</sup> A similar mPPE with amine and ether functional groups was studied by Arnt and Tew.<sup>56</sup> <sup>h</sup> The acid functionalized mPPE was reported by Li et al.<sup>60</sup>

that mPPEs are generally *more* likely to fold in nonpolar solvents, such as hexane and diethyl ether, than in polar solvents like acetonitrile or acetone. This exception even applies to some mPPEs with functional groups of high to moderate polarity, such as the amines, amides, and alcohols. Many of these same polar functionalized mPPEs were found to favor extended conformations in the more polar solvents. This is rather unexpected, since the helical structures should be stabilized by their presumably solvophilic coat of polar functional groups, as proposed earlier.<sup>1,2,15</sup>

Polarity and dielectric considerations also do not suffice to explain why most mPPEs did not exhibit secondary structure in chloroform. Among the 20 functionalized mPPEs in this study, 19 were clearly unable to form a stable helical structure in chloroform, which is in agreement with experimental data that chlorinated solvents do not favor helical mPPE conformations. Yet, many of these exhibited at least partial folding in acetonitrile, acetone, diethyl ether, and hexane, representing solvents of both greater and lesser polarity than chloroform.<sup>61</sup> This confirms previous assertions that strong CH/ $\pi$  interactions between chloroform and mPPE aromatic groups uniquely stabilize disordered mPPE conformations.<sup>14,21,24</sup> Our data suggests only one exception to this behavior, the amide functionalized mPPE (*R* = 4), which showed partial folding behavior (group 3) in chloroform. This anomalous behavior likely results from strong hydrogen bonds that form between the amide functional groups of overlapping residues, as observed during simulations of the amide functionalized polymer in its helical conformation. For every other solvent studied, a wide range of folding behaviors were observed over the set of mPPEs.

The simulation results in Table 3 indicate that, while secondary structure formation is sensitive to solvent conditions, many mPPEs exhibit fairly consistent folding behaviors in a range of solvent environments. For example, out of the 20 mPPEs studied, the ester functionalized mPPE (*R* = 7) showed the most consistent bias toward the folded state, falling into group 4 in all solvents but chloroform. Three other mPPEs (*R* = 10, 11, and 17) showed an equally consistent

bias, but toward the unfolded state. These results suggest that each mPPE possesses some innate tendency to fold or remain disordered, independent of the solvent type. One may conclude that intramolecular interactions within the polymers have a slightly stronger effect on secondary structure formation than do the intermolecular solvent–polymer interactions, though clearly most mPPEs show variation with respect to both.

A key intramolecular interaction for helix formation in mPPEs is the  $\pi$ -stacking between aromatic rings, and it is well-known that this interaction is affected by the electron withdrawing or donating character of the aromatic substituents.<sup>2,5</sup> Although the OPLS force field employs a classical point-charge model, it has been shown to reproduce  $\pi$ -stacking energies in substituted aromatics quite well, in some cases better than high level quantum mechanics computations.<sup>45,55</sup> Simulation results did indicate a reasonable correlation between the deactivating quality of functional groups and their respective mPPE folding behaviors. All mPPEs with deactivating functional groups, to a certain degree, showed a tendency to form more compact conformations. On the other hand, only a few of the mPPEs having activating functional groups were able to form helical structures in any of the solvents. Nearly all helix forming mPPEs (group 4) in Table 3 have deactivating functional groups, with the only exception being the alcohol functionalized mPPE (*R* = 12), which was predicted to fold only in hexane.

It is rather curious that, despite the general trend with respect to electron withdrawing/donating substituents, the two most strongly deactivating functional groups (*R* = 1 and 2) exhibited only partial folding in most simulations, or remained unfolded. According to conventional thought, the presence of these groups should enhance the  $\pi$ -stacking interactions, further increasing the stability of the helical structures. These unexpected results bear more similarity to the simulation results of Blatchly and Tew,<sup>62</sup> in which the stability of  $\pi$ -stacking interactions in *o*-PPEs was found to be stronger between aromatic rings with activating substituents than between rings with deactivating substituents.

The folding behaviors of halide functionalized mPPEs ( $R = 17, 18, 19, 20$ ) were considered separately from the other mPPEs, because of the unique nature of halide functional groups on aromatic rings. These groups have weak deactivating effects, yet still direct substituents to *ortho* and *para* positions in aromatic substitution reactions.<sup>58</sup> A distinct trend was observed in folding behaviors of halide functionalized mPPEs in solvents other than chloroform. The fluoride substituent ( $R = 17$ ) showed group 1 behavior in all five solvents, similar to mPPEs with  $R = 10$  and 11. Yet, when changing the aromatic substituents from fluoride ( $R = 17$ ) to iodine ( $R = 20$ ), the behavior generally shifts toward groups 3 and 4. This shift correlates well with the atomic weight of the halides, as do other properties of the halide functional groups, such as electronegativities, van der Waals radii, and van der Waals interaction energies. In the OPLS force field, Lennard-Jones radius ( $\sigma$ ) parameters for the halide substituents vary from 2.85 Å for fluoride to 3.67 Å for iodide, while the well depths ( $\epsilon$ ) increase from 0.25 to 2.4 kJ/mol. Thus, for the higher molecular weight halides, the position of the potential energy well becomes closer to the separation distance  $R_b$  between aromatic rings, while the energy of the interaction becomes more favorable. These effects stabilize the helical conformation and promote folding for mPPEs containing the heavier halides.

## Summary and Conclusions

In this work, REMD simulations using the OPLS force field were applied as a tool for predicting the most stable conformation of many mPPE variations in different solvents. For each mPPE/solvent pair, two REMD simulations were conducted, one initialized with the oligomer in an extended conformation and the other with a helical conformation, and the simulation results compared to evaluate and categorize the respective mPPE folding behavior. The total time needed for each simulation was modest (10 ns of replica exchange dynamics), allowing us to use this procedure as a quick and simple screening test in a large scale combinatorial study. Our simulation results are in excellent agreement with available data regarding the folding behavior of mPPEs in different solvents. Furthermore, the predictive ability of this REMD protocol was demonstrated for the folding behaviors of two newly synthesized mPPE structures in chloroform and acetonitrile.

The REMD procedure was used to study the folding behavior of 20 uniquely functionalized mPPEs in five explicit solvents, including chloroform, acetonitrile, acetone, diethyl ether, and hexane. The results were categorized into four groups, ranging from group 1, when folding is deemed unlikely, to group 4, when folding is deemed extremely likely. Our compiled results provide evidence that polymer/solvent interactions have a significant influence over the formation of secondary structure, though folding seems to be influenced to a larger degree by the intramolecular interactions within mPPEs. Our simulations showed that electron withdrawing functional groups on the aromatic rings generally promote folding, which is consistent with previous findings. Yet, our results also predict that nonpolar solvents generally promote folding in more cases than for polar solvents, and this finding is counter to the current understanding of the folding mechanism as a process of solvophobic collapse.

Many exceptions were found to the general trends outlined above, due to the often competing effects of solvophobic/solvophilic interactions,  $\pi$ -stacking effects, and other site-specific interactions. A prime example of such an exception is the folding behavior in chloroform; only one out of the 20 mPPEs in this study was found to even partially fold in chloroform, although several polymers showed clear signs of stable secondary structure

in both more polar and less polar solvents. Hence, secondary structure formation in mPPEs is not easily predicted by simple heuristics, and this complex nature of the folding problem suggests that molecular simulation (and particularly the REMD method described here) is an effective tool for predicting whether mPPE helical secondary structures will be stabilized in a given mPPE/solvent combination.

**Acknowledgment.** This study was supported by National Science Foundation, under award number CTS-0626143. The authors would like to acknowledge the support of the staff at Clemson University's Cyber Infrastructure Technology Integration (CITI) group, for administration and maintenance of the computers used in the work. The authors also would like to thank several colleagues for their assistance and use of their experimental equipment, specifically, Dr. John Kaup for use of the fluorescence spectrophotometer, Dr. Christopher Kitchens for use of the UV/vis spectrophotometer, Dr. Alex Kitaygorodskiy for NMR support, and Kim Ivey for use of the GPC.

**Supporting Information Available:** Figures showing raw REMD simulation data for Figures 4, 6, 7, and 8, so as to show the true dynamics of the simulation parameters (e.g., SASA,  $R_g$ , Lennard-Jones interactions energies) and text giving detailed synthesis (including structures) and characterization information for the two mPPEs (21 and 22) described in the paper. This material is available free of charge via the Internet at <http://pubs.acs.org>.

## References and Notes

- (1) Nelson, J. C.; Saven, J. G.; Moore, J. S.; Wolynes, P. G. *Science* **1997**, 277 (5333), 1793–1796.
- (2) Lahiri, S.; Thompson, J. L.; Moore, J. S. *J. Am. Chem. Soc.* **2000**, 122, 11315–11319.
- (3) Stone, M. T.; Fox, J. M.; Moore, J. S. *Org. Lett.* **2004**, 6, 3317–3320.
- (4) Stone, M. T.; Heemstra, J. M.; Moore, J. S. *Acc. Chem. Res.* **2006**, 39, 11–20.
- (5) Hill, D. J.; Mio, M. J.; Prince, R. B.; Hughes, T. S.; Moore, J. S. *Chem. Rev.* **2001**, 101, 3893–4011.
- (6) Heemstra, J. M.; Moore, J. S. *Org. Lett.* **2004**, 6, 659–662.
- (7) Adisa, B.; Bruce, D. A. *J. Phys. Chem. B* **2005**, 109, 7548–7556.
- (8) Adisa, B.; Bruce, D. A. *J. Phys. Chem. B* **2005**, 109, 19952–19959.
- (9) Elmer, S. P.; Park, S.; Pande, V. S. *J. Chem. Phys.* **2005**, 123, 114903.
- (10) Elmer, S.; Pande, V. S. *J. Phys. Chem. B* **2001**, 105, 482–485.
- (11) Lee, O. S.; Saven, J. G. *J. Phys. Chem. B* **2004**, 108, 11988–11994.
- (12) Elmer, S. P.; Pande, V. S. *J. Chem. Phys.* **2004**, 121, 12760–12771.
- (13) Elmer, S. P.; Park, S.; Pande, V. S. *J. Chem. Phys.* **2005**, 123, 114902.
- (14) Hill, D. J.; Moore, J. S. *Proc. Natl. Acad. Sci. U.S.A.* **2002**, 99, 5053–5057.
- (15) Ray, C. R.; Moore, J. S., *Supramolecular Organization of Foldable Phenylene Ethynylene Oligomers*. In *Poly(Arylene Ethynylene)s: From Synthesis to Application*, 2005; Vol. 177, pp 91–149.
- (16) Tan, C. Y.; Pinto, M. R.; Kose, M. E.; Ghiviriga, I.; Schanze, K. S. *Adv. Mater.* **2004**, 16, 1208.
- (17) Podeszwa, R.; Szalewicz, K. *Phys. Chem. Chem. Phys.* **2008**, 10, 2735–2746.
- (18) Sinnokrot, M. O.; Sherrill, C. D. *J. Phys. Chem. A* **2003**, 107, 8377–8379.
- (19) Sinnokrot, M. O.; Sherrill, C. D. *J. Am. Chem. Soc.* **2004**, 126, 7690–7697.
- (20) Tsuzuki, S.; Honda, K.; Uchimaru, T.; Mikami, M.; Fujii, A. *J. Phys. Chem. A* **2006**, 110, 10163–10168.
- (21) Nishio, M.; Hirota, M.; Umezawa, Y. *The CH- $\pi$  interaction: evidence, nature, and consequences*; Wiley: New York, 1998; p 217.
- (22) Arnstein, S. A.; Sherrill, C. D. *Phys. Chem. Chem. Phys.* **2008**, 10, 2646–2655.
- (23) Lee, E. C.; Hong, B. H.; Lee, J. Y.; Kim, J. C.; Kim, D.; Kim, Y.; Tarakeshwar, P.; Kim, K. S. *J. Am. Chem. Soc.* **2005**, 127, 4530–4537.
- (24) Tsuzuki, S.; Honda, K.; Uchimaru, T.; Mikami, M.; Tanabe, K. *J. Phys. Chem. A* **2002**, 106, 4423–4428.
- (25) Sugita, Y.; Okamoto, Y. *Chem. Phys. Lett.* **1999**, 314, 141–151.

- (26) Beck, D. A. C.; White, G. W. N.; Daggett, V. *J. Struct. Biol.* **2007**, *157*, 514–523.
- (27) Periolo, X.; Mark, A. E. *J. Chem. Phys.* **2007**, *126*, 014903.
- (28) Seibert, M. M.; Patriksson, A.; Hess, B.; van der Spoel, D. *J. Mol. Biol.* **2005**, *354*, 173–183.
- (29) Zhang, W.; Wu, C.; Duan, Y., *J. Chem. Phys.* **2005**, *123*, 154105.
- (30) Van der Spoel, D.; Lindahl, E.; Hess, B.; Groenhof, G.; Mark, A. E.; Berendsen, H. J. C. *J. Comput. Chem.* **2005**, *26*, 1701–1718.
- (31) Lindahl, E.; Hess, B.; van der Spoel, D. *J. Mol. Model.* **2001**, *7*, 306–317.
- (32) Berendsen, H. J. C.; van der Spoel, D.; Vandrunen, R. *Comput. Phys. Commun.* **1995**, *91*, 43–56.
- (33) GROMACS USER MANUAL. <http://www.gromacs.org/Documentation/Manual>.
- (34) Bekker, H.; Dijkstra, E. J.; Berendsen, H. J. C. *Supercomputer* **1993**, *10* (2), 4–10.
- (35) Hess, B.; Bekker, H.; Berendsen, H. J. C.; Fraaije, J. *J. Comput. Chem.* **1997**, *18*, 1463–1472.
- (36) Hukushima, K.; Nemoto, K. *J. Phys. Soc. Jpn.* **1996**, *65*, 1604–1608.
- (37) *Materials Studio*, v. 4.4, Accelrys Software Inc.: San Diego, CA, **2008**.
- (38) Berendsen, H. J. C.; Postma, J. P. M.; Vangunsteren, W. F.; Dinola, A.; Haak, J. R. *J. Chem. Phys.* **1984**, *81*, 3684–3690.
- (39) Parrinello, M.; Rahman, A. *J. Appl. Phys.* **1981**, *52*, 7182–7190.
- (40) Patriksson, A.; van der Spoel, D. *Phys. Chem. Chem. Phys.* **2008**, *10*, 2073–2077.
- (41) Humphrey, W.; Dalke, A.; Schulten, K. *J. Mol. Graphics* **1996**, *14* (1), 33–38.
- (42) Eisenberg, D.; McLachlan, A. D. *Nature* **1986**, *319* (6050), 199–203.
- (43) Eisenhaber, F.; Lijnzaad, P.; Argos, P.; Sander, C.; Scharf, M. *J. Comput. Chem.* **1995**, *16*, 273–284.
- (44) *High performance computing*. <http://citi.clemson.edu/hpc>.
- (45) Jorgensen, W. L.; Maxwell, D. S.; TiradoRives, J. *J. Am. Chem. Soc.* **1996**, *118*, 11225–11236.
- (46) Jorgensen, W. L. *J. Phys. Chem.* **1986**, *90*, 1276–1284.
- (47) Jorgensen, W. L.; Madura, J. D.; Swenson, C. J. *J. Am. Chem. Soc.* **1984**, *106*, 6638–6646.
- (48) Sinnokrot, M. O.; Valeev, E. F.; Sherrill, C. D. *J. Am. Chem. Soc.* **2002**, *124*, 10887–10893.
- (49) Lide, D. R.; Kehiaian, H. V. *CRC Handbook of Thermophysical and Thermochemical Data*; CRC Press: Boca Raton, FL, 1994.
- (50) Torres, R. B.; Francesconi, A. Z.; Volpe, P. L. O. *Fluid Phase Equilib.* **2002**, *200* (1), 1–10.
- (51) Yang, W. Y.; Prince, R. B.; Sabelko, J.; Moore, J. S.; Gruebele, M. *J. Am. Chem. Soc.* **2000**, *122*, 3248–3249.
- (52) Stone, M. T.; Moore, J. S. *Org. Lett.* **2004**, *6*, 469–472.
- (53) Adams, H.; Hunter, C. A.; Lawson, K. R.; Perkins, J.; Spey, S. E.; Urch, C. J.; Sanderson, J. M. *Chem.—Eur. J.* **2001**, *7*, 4863–4877.
- (54) Cockroft, S. L.; Hunter, C. A.; Lawson, K. R.; Perkins, J.; Urch, C. J. *J. Am. Chem. Soc.* **2005**, *127*, 8594–8595.
- (55) Sherrill, D. C., Computations of Noncovalent pi-interactions. In *Reviews in computational chemistry*; Lipkowitz, K. B., Boyd, D. B., Eds. Wiley: New York, 2009; Vol. 26, pp 1–30.
- (56) Arnt, L.; Tew, G. N. *J. Am. Chem. Soc.* **2002**, *124*, 7664–7665.
- (57) Prince, R. B.; Saven, J. G.; Wolynes, P. G.; Moore, J. S. *J. Am. Chem. Soc.* **1999**, *121*, 3114–3121.
- (58) Carey, F. A.; Sundberg, R. J. *Advanced organic chemistry, Part A: Structure and Mechanisms*, 5th ed.; Springer: New York, 2007.
- (59) Brunsveld, L.; Prince, R. B.; Meijer, E. W.; Moore, J. S. *Org. Lett.* **2000**, *2*, 1525–1528.
- (60) Li, C. J.; Slaven, W. T.; Chen, Y. P.; John, V. T.; Rachakonda, S. H. *Chem. Commun.* **1998**, 1351–1352.
- (61) Reichardt, C., *Solvents and solvent effects in organic chemistry*, 3rd ed.; Wiley-VCH: Weinheim, Germany, and Cambridge, U.K., 2003; p 640.
- (62) Blatchly, R. A.; Tew, G. N. *J. Org. Chem.* **2003**, *68*, 8780–8785.